The effects of chopper jitter on the time-dependent intensity transmitted by multiple-slot multiple disk chopper systems

J. R. D. Copley
University of Maryland
College Park, Maryland 20742
and
National Institute of Standards and Technology
Gaithersburg, Maryland 20899
USA

ABSTRACT: We present Monte Carlo calculations of the time dependence of the intensity transmitted by single- and multiple-slot multiple disk chopper assemblies, taking into account the effects of chopper jitter. In the case of multiple-slot systems, where each of at least two choppers and a mask is fitted with two or more slots, a switching function is employed to suppress contaminated pulses, i.e., pulses in which neutrons can pass through slots that would never line up in the absence of jitter. Such pulses, if accepted, would degrade the time resolution of the system. Our results for the time-integrated intensity are in good agreement with previously reported semi-analytic calculations. The need to reject contaminated pulses in multiple-slot systems is emphasized.

Introduction

One of the standard ways to pulse a thermal neutron beam is to use a disk chopper spinning about an axis parallel to the beam[1]. The burst time and the intensity transmitted by this type of device depend, *inter alia*, on the width of the beam, the width of the slot in the chopper, and the speed with which the slot passes through the beam. In very high-resolution (short burst time) applications, the slot is narrower than the beam, and the beam is masked down to the width of the slot, as shown in Fig. 1(a), in order to achieve the desired performance. (It is assumed throughout this discussion that the chopper is turning at maximum speed.)

A necessary consequence of the masking of the beam is a reduction in the transmitted intensity, but the intensity can be effectively doubled, with no change in the burst time, using two counter-rotating choppers and, at the same time, doubling the slot widths in the choppers and the mask, as illustrated in Fig. 1(b). This idea is employed in the MIBEMOL spectrometer at the Orphee reactor[2] and in the time-of-flight spectrometer that is presently under construction at the Hahn-Meitner Institut reactor in Berlin[3].

A further doubling in intensity (with no change in burst time) is, in principle, achievable[4] using two counter-rotating choppers and a stationary mask, each fitted with two slots whose centres are separated by a distance that is at least twice the

width of the individual slots (Fig. 1(c)). This concept can be extended still further with the next stage being a system of three choppers and a mask, each fitted with four slots, as shown in Fig. 1(d): in this case the relative speeds of the choppers are +1, -1, and 1/2, and again the intensity is doubled with no change in the burst time of the system.

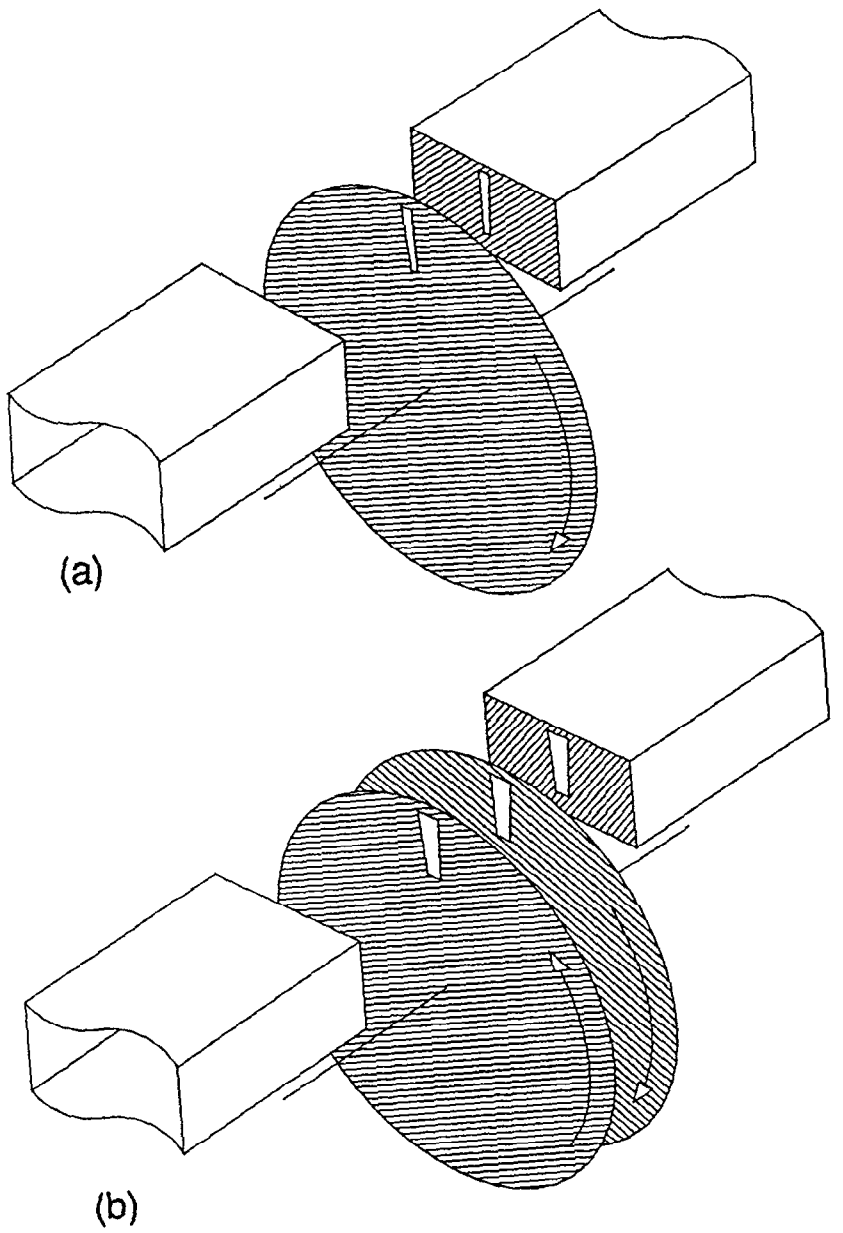

Fig. 1 (continued on next page).

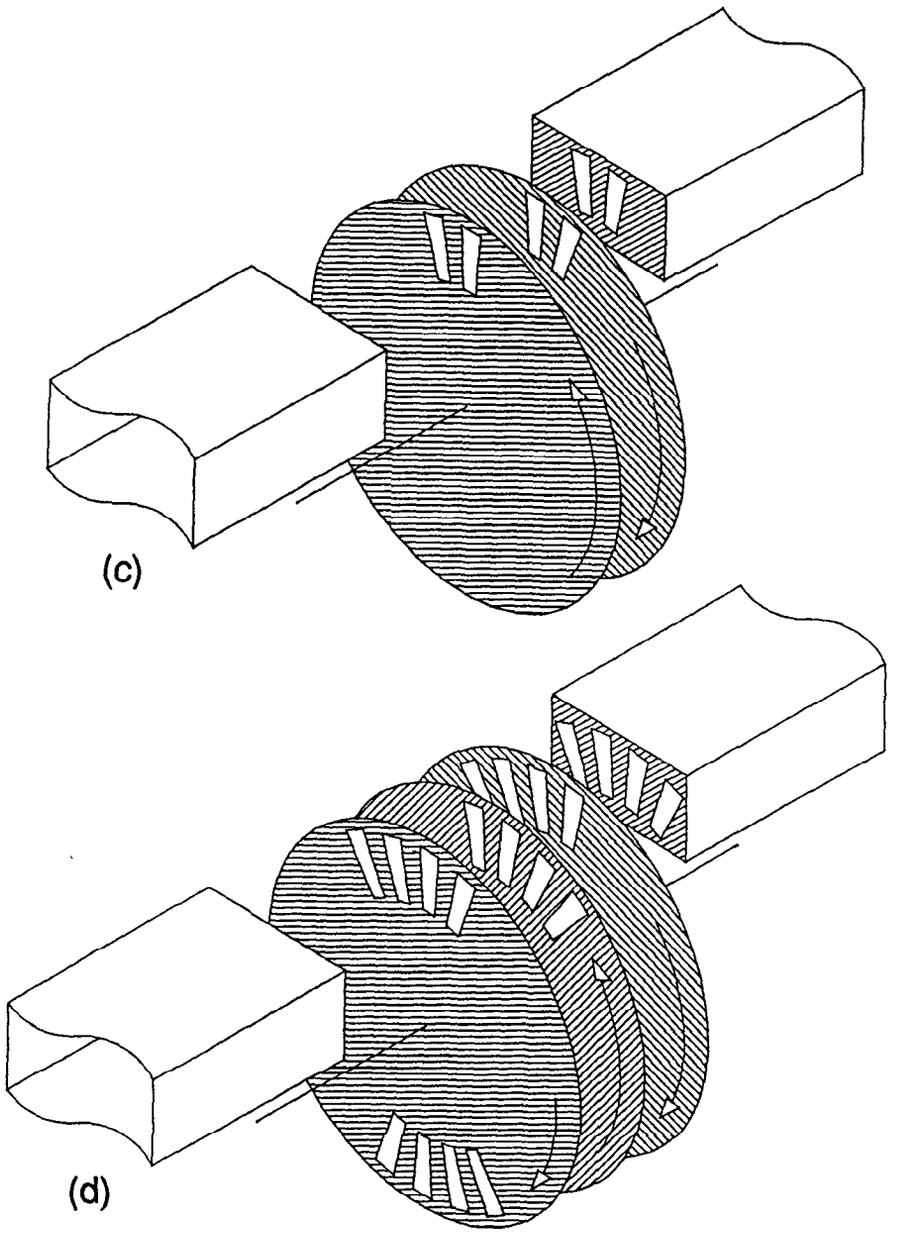

Fig. 1 Schematic views of several chopper assemblies. The width of the neutron guide is exaggerated for clarity. In (a) the single-slot single chopper arrangement is shown: note that the slots are one-half the width of the slots in the other systems. The one-slot and two-slot two chopper setups are shown in (b) and (c) respectively. The four-slot three chopper arrangement is illustrated in (d): in this case the third chopper is spinning at one-half the speed of the other choppers. It is fitted with a second set of slots so that there is still one pulse per revolution of the faster choppers.

The gains in intensity described in the previous two paragraphs only occur if the overall width of the slot system is no greater than the available beam width and if the choppers remain exactly phased. In practice the choppers jitter, causing phase deviations to occur, and in the remainder of this paper we shall discuss the consequences of this departure from ideal behaviour.

In a previous paper[4] we described semi-analytic calculations of the effects of chopper phase deviations on the transmitted intensity in the two-slot two chopper and the four-slot three chopper systems. Here we shall describe Monte Carlo calculations which, though less accurate and in some cases much more time-consuming, are very much easier to formulate and code. The time dependence of the transmitted intensity is calculated, and the total intensity per pulse is obtained by integration over time.

Calculations

Whereas the semi-analytic calculations[4] were formulated in dimensionless units, the present Monte Carlo calculations are expressed in real units. We consider 50-cm diameter disks spinning at 19,100 rpm (9,550 rpm for the slower chopper in the three chopper system), with slots of full width 0.5 cm (0.25 cm for the single chopper system) and negligible radial extent, placed on the circumference of the disk. The peripheral velocity V of the slots in the faster choppers is therefore 500 m/s, and the burst time is 5 μs (full width at half maximum height, FWHM). We assume that the separation between the disks in the multiple chopper systems may be neglected.

In order to define phasing deviations, we postulate a reference clock with fixed period T_0. Each disk, labelled k, is fitted with a magnetic spot that is detected by a fixed pickup at times $t_\kappa(i) = \Delta t_\kappa + iT_0 + \delta t_\kappa(i)$, where Δt_κ is a constant delay, i is an integer, and $\delta t_\kappa(i)$ is the time deviation of the i'th pulse. The function that defines the probability that δt_κ has the value x is assumed to be the (normalized) Gaussian function $G(\sigma_\kappa|x)$, which has zero mean and standard deviation σ_κ. With no loss in generality, we may mentally position the magnetic spots and pickups so that $\Delta t_\kappa = 0$ for each disk.

Before proceeding any further we need to explain the concept of contaminated pulses in multiple-slot chopper systems. As an example we consider the two-slot system illustrated in Fig. 1(c). The movement of the slots in the choppers (and the lack of movement of the slots in the mask) is illustrated in Fig. 2(a), for the case of perfect phasing ($\delta t_1 = \delta t_2 = 0$). If both choppers are delayed the same length of time (i.e., if $\delta t_1 = \delta t_2 \neq 0$), the intensity is unchanged, but the burst does not occur at the intended time. If the delays are different, as illustrated in Fig. 2(b), there is in general a decrease in the intensity of the two principal components and an associated appearance of intensity in two satellite components. Principal and satellite components are due to neutrons that, respectively, do and do not pass through corresponding slots in the choppers and the mask. A contaminated pulse is defined to be a pulse that has a non-zero satellite component to the intensity. If the width of a slot is 2b and the center-to-center slot separation is 2B, then if B = 2b all pulses with non-zero relative time deviation must be contaminated and, therefore, unacceptable. To reduce the likelihood of a contaminated pulse it is necessary to

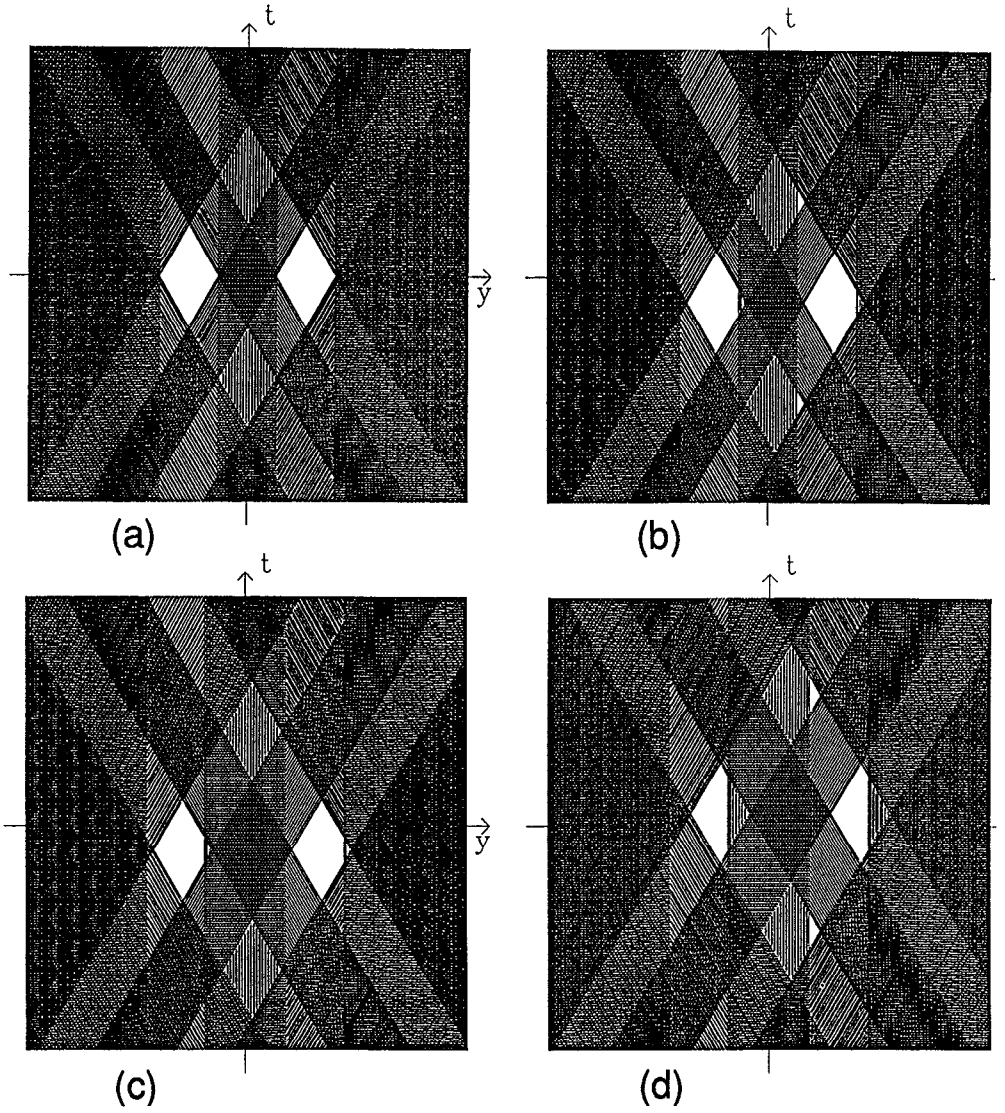

Fig. 2 Diagrams illustrating tangential chopper displacements y as a function of time t for the two-slot two chopper system illustrated in Fig. 1(c). In (a) and (b) the center-to-center slot separation 2B is exactly twice the slot width 2b, whereas in (c) and (d) the ratio χ, i.e., B/2b, is greater than unity. In (a) the choppers are exactly phased but in (b) they are not, and satellite intensity is evident: the pulse is contaminated. In (c) the phase deviations are the same as in (b), but there is no satellite intensity because of the increased value of χ. On the other hand, the phase deviations in (d) are sufficiently large that the pulse is contaminated.

make B somewhat greater than 2b. There is then a range of relative time deviations for which no contamination occurs, whereas contaminated pulses will be produced if the relative time deviation is sufficiently great, as indicated in Figs. 2(c) and 2(d). In order to exclude the possibility of degradation of the resolution by contaminated pulses, the phases of the choppers should be continuously monitored, and contaminated pulses should be rejected by the data acquisition system. Similar considerations apply to the case of the three chopper system illustrated in Fig. 1(d).

The rejection of contaminated pulses may be mathematically represented by a switching function, as has been previously discussed[4]. For the two-slot two chopper system the function is unity for $|\xi| < \chi - 1$, where $\xi = -V(\delta t_1 - \delta t_2)/4b$ and $\chi = B/2b$, and otherwise it is zero. For the four-slot three chopper system it is unity if one or the other of the following sets of conditions is satisfied:

(i) $|\xi| < \chi^{-1}$ and $\xi\zeta > 0$ and $|(\xi+\zeta)/2| < \chi^{-1}$
(ii) $|\xi| < \chi^{-1}$ and $\xi\zeta \leq 0$ and $|(2\xi+\zeta)/2| < \chi^{-1}$.

Here $\zeta = -V(\delta t_1 + \delta t_2 - 2\delta t_3)/4b$. If neither of these conditions is satisfied, the switching function is zero.

The first step in each of the calculations was to select standard deviations σ_κ for each of the choppers. Standard deviations were made equal for choppers rotating at the same speed (i.e., σ_2 was made equal to σ_1), whereas the standard deviation for the slower chopper in the three chopper system was assumed to be either the same as, or else twice that of, the faster choppers (i.e., σ_3/σ_1 was set to either 1 or 2): the latter choice is equivalent to making the standard deviations of the angular distributions of the three choppers identical. A time deviation δt_κ was then selected for each of the choppers from the appropriate Gaussian distribution, and the transmission of the system was computed as a function of time. The procedure was repeated many times, for different choices of the time deviations δt_κ, in order to achieve the desired statistical precision. Calculations were made either with respect to the reference clock or with respect to the mean delay time of the pickup pulses from the choppers (ignoring that of the slower chopper in the case of the three chopper system). In the case of multiple-slot systems, time distributions were computed for various choices of the parameter χ, and calculations were performed both with and without the contaminated pulse-switching function described above.

Results

We shall use $I_C(\sigma,t)$ and $I_P(\sigma,t)$ to denote transmitted intensities, time being measured with respect to the reference clock and with respect to the mean pickup pulse (as described above), respectively. The corresponding time-integrated intensities $I_C(\sigma)$ and $I_P(\sigma)$ are identical, and the shorter notation $I(\sigma)$ will be used. We shall drop the subscript on σ except in cases where doing so would introduce ambiguity.

For all systems examined with the contaminated-pulse-switching function activated, $I_P(\sigma,t)$ is only non-zero for time differences less than the burst time of the assembly, whereas $I_C(\sigma,t)$ is (for $\sigma > 0$) a broader function with undesirable tails. For

example, $I_P(\sigma,t)$ for the single chopper system is a triangular distribution with an FWHM of 5 μs, independent of σ; whereas $I_C(\sigma,t)$ is the convolution of $I_P(\sigma,t)$ with $G(\sigma|t)$: $I(\sigma)/I(0) = 1$ for all values of σ. In view of the above it is clearly advisable (and it is normal practice) to relate the start time of a data acquisition cycle to the mean pickup pulse rather than to the system clock. We shall not discuss $I_C(\sigma,t)$ any further.

The function $I_P(\sigma,t)$ for the single-slot two chopper system is shown in Fig. 3 for several choices of σ. Similar rounded triangular line shapes are found for the time distributions $I_P(\sigma,t)$ for all of the multiple-slot systems we have studied. For example, Fig. 4(a) shows results for the two-slot two chopper system with $\chi = 1.1$: note that as σ is increased, the intensity drops more rapidly than in the case of the one-slot two chopper system shown in Fig. 3. In Fig. 4(b) we show time distributions for the same system, for $\sigma = 1$ μs and $\sigma = 2$ μs, with and without the contaminated-pulse-switching function activated. The switching function reduces the transmitted intensity significantly, but little intensity appears in the satellites if it is turned off. For example, the integrated intensity ratio $I_P(\sigma)/I_P(0)$ is reduced from ~0.99 to ~0.83 when $\sigma = 1$ μs (~0.97 to ~0.53 when $\sigma = 2$ μs), but the contribution to the integrated intensity in the satellites (with the switching function turned off) is only ~0.0006 (~0.012). This is because the switching function rejects all contaminated pulses, even though almost all of the intensity in these pulses is in the principal component.

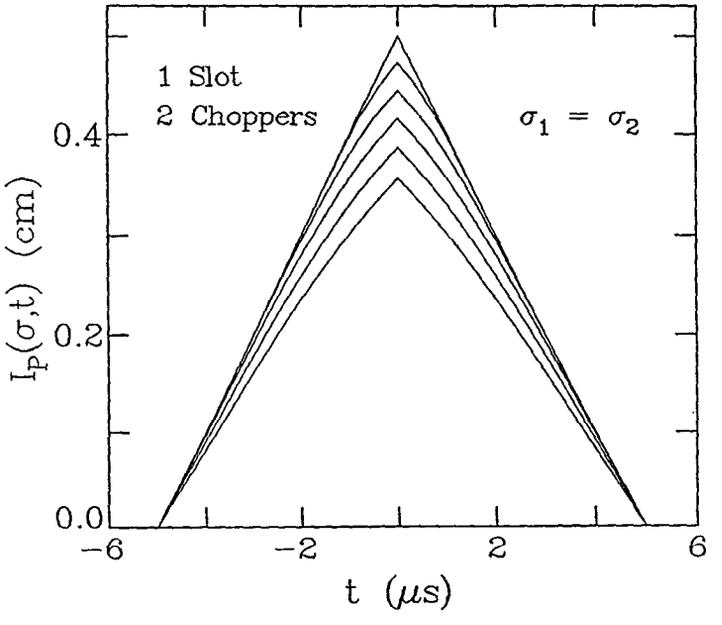

Fig. 3 Transmitted intensities Ip(σ,t) for the single-slot two chopper system. The intensity is expressed in units of length. For example, when σ = 0 and t = 0, neutrons are transmitted over the full width of the slots, 0.5 cm. Successive plots, starting from the top, correspond to s = 0, 1, 2, 3, 4, and 5 μs.

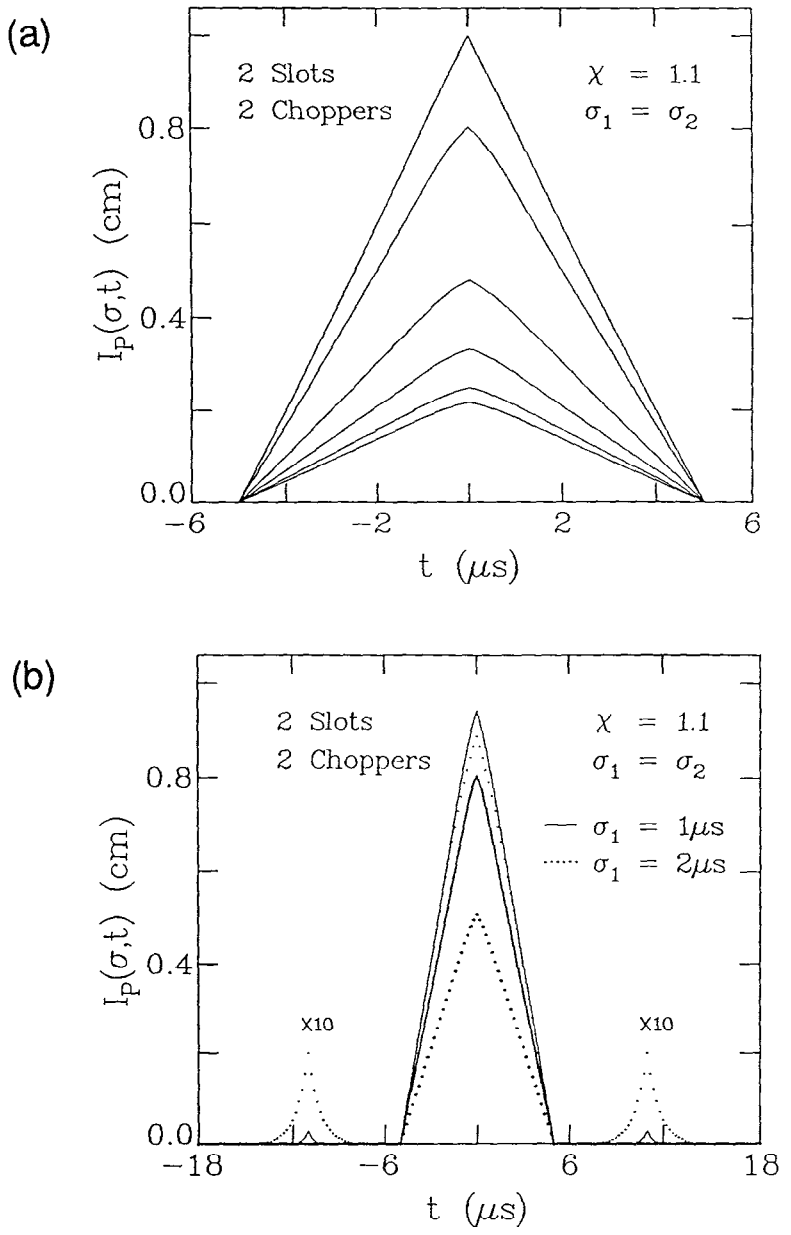

Fig. 4 Transmitted intensities Ip(σ,t) for the two-slot two chopper system. The unit of intensity is explained in the caption to Fig. 3. Results for $\chi = 1.1$ are shown in (a). Successive plots, starting from the top, correspond to $\sigma = 0$, 1, 2, 3, 4, and 5 μs. Intensities for $\chi = 1.1$, for $\sigma = 1$ μs and $\sigma = 2$ μs, are shown in (b). The darker and lighter lines represent the results of calculations where the contaminated pulse switching function is on and off, respectively. The scale of the satellite intensities is increased by a factor of 10 to make them more apparent.

Integrated intensities for the two-slot two chopper system are compared with our earlier semi-analytic results in Fig. 5: the agreement is good. The ratio $I(\sigma)/I(0)$ for the one-slot two chopper system is identical to $I(\sigma)/I(0)$ for the two-slot two chopper system with $\chi = \infty$, being the convolution of the function $f_1(\xi)$, introduced in reference 4 (appendix 1), with $G(\sigma|\xi)$. In Table 1 we present selected results for $I(\sigma)/I(0)$ for the two-slot system, derived from the semi-analytic calculations.

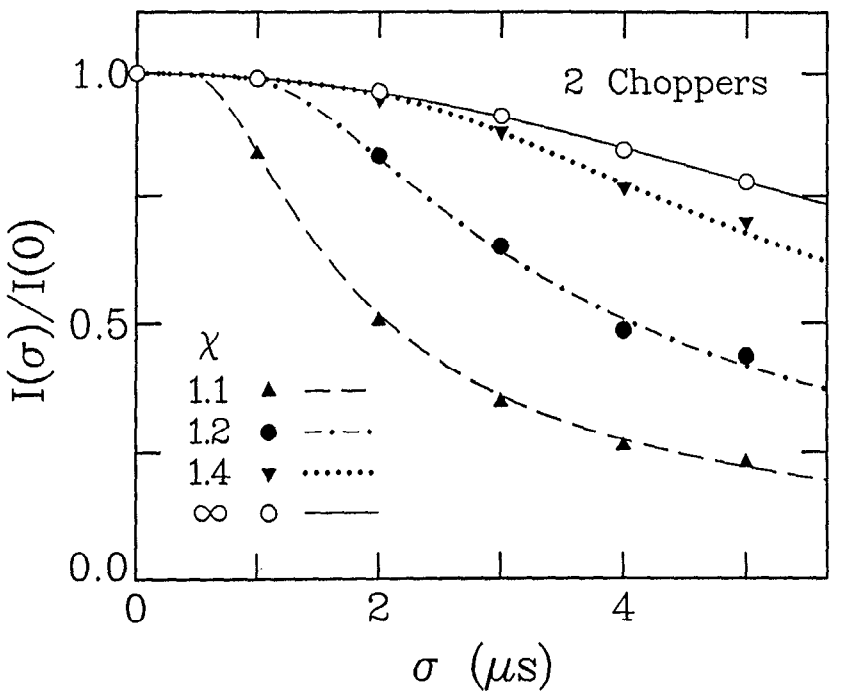

Fig. 5 The time-integrated intensity ratio for the two-slot two chopper system, for various choices of χ. The symbols represent the present Monte Carlo calculations whereas the lines show the results of earlier semi-analytic calculations[4]. The line labelled $\chi = \infty$ also represents the integrated intensity ration for the single-slot two chopper system.

In Fig. 6 we show results for $I_P(\sigma,t)$, for the four-slot three chopper system with $\sigma_3 = \sigma_1 = 1$ μs and 2 μs and $\chi = 1.1$, with and without the contaminated-pulse-switching function activated: again the switching function reduces the intensity very significantly, but there is little intensity in the satellites when the switching function is turned off. Intensity ratios $I(\sigma)/I(0)$ for this system, for $\sigma_3/\sigma_1 = 1$ and 2, are again in good agreement with the earlier semi-analytic calculations, and selected results from the latter calculations are given in Table 2.

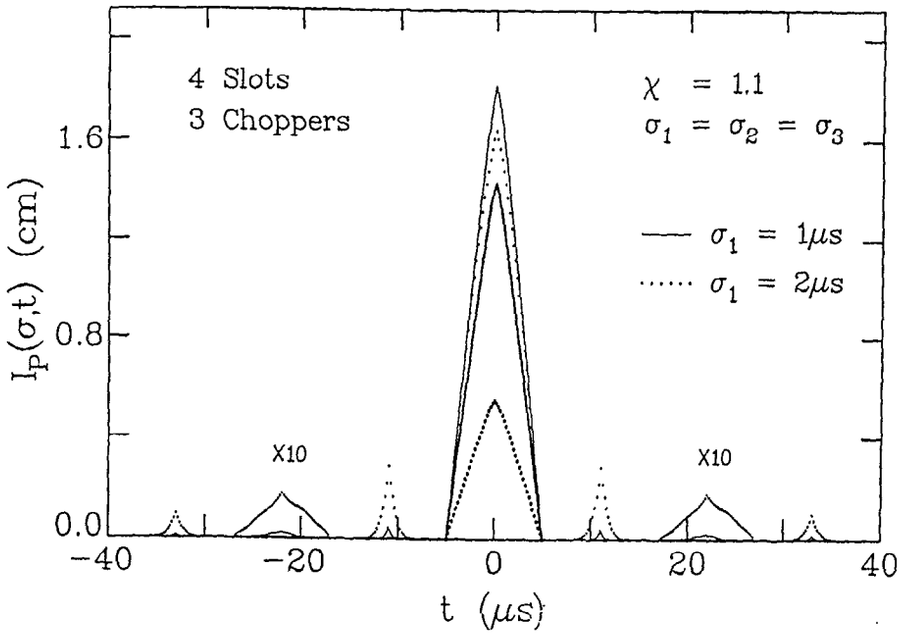

Fig. 6 The time-dependent intensity Ip(σ,t) for the four-slot three chopper system with $\chi = 1.1$, $\sigma_1 = \sigma_3$, and $\sigma_1 = 1\ \mu s$ and $\sigma_1 = 2\ \mu s$. The darker and lighter lines represent the results of calculations, where the contaminated-pulse-switching function is on and off, respectively. The scale of the satellite intensities is increased by a factor of 10 to make them more apparent. The unit of intensity is explained in the caption to Fig.3.

Table 1. Values of the integrated intensity ratio for the two-slot two chopper system for selected values of $\chi = B/2b$. The column for $\chi = \infty$ also represents the integrated intensity ratio for the single-slot two chopper system. The quantity σ_ξ is given[4] by $\sigma_\xi^2 = (V/4b)^2(\sigma_1^2 + \sigma_2^2)$ so that, for the system studied in this paper, $\sigma_1 = 14.14\sigma_\xi$ μs.

χ / σ_ξ	1.100	1.200	1.300	1.400	∞
0.00	1.000	1.000	1.000	1.000	1.000
0.02	0.999	0.999	0.999	0.999	0.999
0.04	0.985	0.997	0.997	0.997	0.997
0.06	0.900	0.992	0.993	0.993	0.993
0.08	0.785	0.976	0.987	0.987	0.987
0.10	0.679	0.940	0.978	0.980	0.980
0.12	0.592	0.888	0.962	0.971	0.971
0.14	0.522	0.830	0.937	0.958	0.961
0.16	0.465	0.772	0.904	0.942	0.949
0.18	0.419	0.717	0.867	0.920	0.935
0.20	0.381	0.667	0.828	0.895	0.920
0.24	0.321	0.581	0.750	0.838	0.887
0.28	0.277	0.512	0.679	0.779	0.850
0.32	0.244	0.456	0.617	0.721	0.811
0.36	0.217	0.411	0.563	0.667	0.772
0.40	0.196	0.373	0.516	0.619	0.734
0.50	0.157	0.303	0.426	0.520	0.645
0.60	0.132	0.254	0.361	0.445	0.570

Table 2. Values of the integrated intensity ratio I(σ)/I(0) for the three chopper system for selected values of $\chi = B/2b$, for $\sigma_3/\sigma_1 = 1$ and 2. The quantity σ_ξ is given[4] by $\sigma_\xi^2 = (V/4b)^2(\sigma_1^2 + \sigma_2^2)$.

χ	1.100	1.200	1.300	1.400	1.100	1.200	1.300	1.400
σ_ξ		$\sigma_3/\sigma_1 = 1$				$\sigma_3/\sigma_1 = 2$		
0.00	1.000	1.000	1.000	1.000	1.000	1.000	1.000	1.000
0.02	0.998	0.998	0.998	0.998	0.995	0.996	0.996	0.996
0.04	0.975	0.992	0.992	0.992	0.884	0.984	0.985	0.985
0.06	0.844	0.979	0.981	0.981	0.677	0.940	0.965	0.966
0.08	0.674	0.946	0.966	0.966	0.497	0.852	0.931	0.940
0.10	0.528	0.880	0.945	0.948	0.367	0.742	0.877	0.906
0.12	0.416	0.795	0.913	0.926	0.278	0.634	0.811	0.863
0.14	0.333	0.705	0.869	0.899	0.215	0.537	0.740	0.813
0.16	0.270	0.621	0.816	0.867	0.171	0.455	0.668	0.759
0.18	0.223	0.546	0.759	0.830	0.138	0.388	0.600	0.704
0.20	0.186	0.481	0.701	0.789	0.114	0.332	0.538	0.649
0.25	0.125	0.354	0.567	0.680	0.075	0.233	0.409	0.525
0.30	0.089	0.268	0.458	0.577	0.053	0.170	0.316	0.424
0.35	0.067	0.208	0.373	0.488	0.039	0.129	0.248	0.344
0.40	0.052	0.165	0.307	0.414	0.030	0.101	0.199	0.283
0.50	0.034	0.110	0.215	0.303	0.020	0.066	0.135	0.197
0.60	0.023	0.079	0.158	0.228	0.014	0.047	0.096	0.144

Discussion

We have described Monte Carlo calculations of the time-dependent intensity and the integrated intensity transmitted by single- and multiple-slot chopper systems. The results of earlier calculations[4] of the integrated intensity are fully confirmed. This in itself justifies the present calculations, since the earlier calculations were quire complicated in their formulation. In the course of the present work, an error was discovered (prior to publication) in one of the equations of reference 4. This lends credence to the argument that Monte Carlo calculations may be used to check analytic calculations, and *vice versa.*

Figures 4(b) and 6 demonstrate the effects of activating the contaminant-pulse-switching function with multiple-slot chopper systems. The loss in intensity is considerable, especially when σ is large; but the pulse is perfectly clean. The satellite peaks, which appear when the switching function is not used, have potentially disastrous implications with respect to the interpretation of time-of-flight data acquired under such circumstances. The best course of action is to use very stable choppers, e.g., with a σ of order 10% or less of the burst time, and to reject all contaminated pulses.

It is our intention to build a high-resolution multiple-disk-chopper time-of-flight spectrometer in the neutron guide hall of the Cold Neutron Research Facility at the National Institute of Standards and Technology (formerly the National Bureau of Standards). The design specification requires burst times of the order of 5 - 10 μs, and the available guide dimensions are such that we may well decide to include an option to use the two-slot double chopper arrangement illustrated in Fig. 1(c). We expect to operate the choppers at a maximum speed of 20,000 rpm, and the mean chopper disk diameter will be of order 50 cm. The calculations described in this paper and in our previous publication[4] suggest that σ for each of the choppers should be no greater than 1 μs if $\chi = 1.2$. Recent measurements[5] of this quantity, using a chopper system build at the KFA (Jülich, Federal Republic of Germany) research center, indicate that values of σ of the order of 50 - 100 ns may be achieved. It, therefore, seems that the necessary technology already exists so that we can exploit the multiple-slot chopper concept and, thereby, realize a significant gain in instrumental throughput.

Acknowledgements

Helpful discussions with R. Lechner, J. Raebiger and J. K. Fremerey are gratefully acknowledged.

References

1. F. Douchin, R. E. Lechner and R. Scherm, (unpublished). For a short description of the IN5 spectrometer see the report Neutron Research Facilities at the ILL High Flux Reactor (Institut Laue-Langevin, Grenoble, France, December 1983, pp. 75-77 (unpublished).
2. S. Hautecler, E. Legrand, L. Vansteelandt, P. d'Hooghe, G. Rooms, A. Seeger, W. Schalt and G. Gobert, 1985, Proc. Conf. Neutron Scattering in the 'Nineties, Jülich, (IAEA, Vienna, 1985) p. 211.
3. R. E. Lechner, private communication.
4. J. R. D. Copley, 1988, Nucl. Instrum. Meth. (in press).
5. J. Raebiger, J. K. Fremerey, R. Lechner and J. R. D. Copley, unpublished results.